Analytica Chimica Acta 945 (2016) 85–94

Contents lists available at ScienceDirect

Analytica Chimica Acta

journal homepage: www.elsevier.com/locate/aca

Multiple signal amplified electrochemiluminescent immunoassay for brombuterol detection using gold nanoparticles and polyamidoamine dendrimers-silver nanoribbon

Tiantian Dong, Liuyi Hu, Kang Zhao, Anping Deng**, Jianguo Li*

The Key Lab of Health Chemistry & Molecular Diagnosis of Suzhou, College of Chemistry, Chemical Engineering & Materials Science, Soochow University, Suzhou 215123, China

HIGHLIGHTS

- A multiple signal amplification ECL immunosensor of eco-friendly CdSe QDs for brombuterol determination was developed.
- Besides substrates, AuNPs and PAMAM-SNR were creatively used to accelerate the electron transport between electrode and QDs.
- SNR-PAMAM with numerous amino groups also could be employed to bond abundant actived QDs to amplify ECL signal.
- Competitive immunoassay was performed with ECL to detect small molecules of brombuterol.
- It provided a method for detecting Brom and enlarged the usage of QDs, AuNPs and SNR-PAMAM in ECL biosensing.

GRAPHICAL ABSTRACT

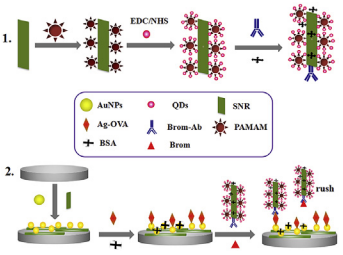

ARTICLE INFO

Article history:
Received 28 July 2016
Received in revised form
27 September 2016
Accepted 3 October 2016
Available online 14 October 2016

Keywords:
Amplification strategy
Electrochemiluminescent immunosensor
CdSe QDs
Silver-cysteine hybrid nanoribbon
Gold nanoparticles
Brombuterol

ABSTRACT

Electrochemiluminescent (ECL) immunosensor with multiple signal amplification was designed based on gold nanoparticles (AuNPs), polyamidoamine dendrimers (PAMAM) and silver-cysteine hybrid nanoribbon (SNR). Low toxic L-cysteine capped CdSe QDs was chosen as the ECL signal probe. To verify the proposed ultrasensitive ECL immunosensor for β-adrenergic agonists (β-AA), we detected Brombuterol (Brom) as a proof-of-principle analyte. Therein, AuNPs as the substrate can simplify the experiment process, accelerate the electron transfer rate, and carry more coating antigen (Ag-OVA) to enlarge ECL signal. On one hand, SNR on the surface of electrode can avoid the aggregation of AuNPs, and SNR-PAMAM-AuNPs also can be acted as a good accelerator for electron transfer. On the other hand, PAMAM (16 -NH_2) functionalized SNR (SNR-PAMAM) with numerous amino groups could be employed to bond abundant actived QDs to further amplify ECL signal. The new immunosensor can offer a simple, reliable, rapid, and selective detection for Brom, which have a dynamic range of 0.005–700 ng mL^{-1} with

* Corresponding author.
** Corresponding author.
E-mail addresses: denganping@suda.edu.cn (A. Deng), lijgsd@suda.edu.cn (J. Li).

http://dx.doi.org/10.1016/j.aca.2016.10.006

a low detection limit at 1.5 pg mL^{-1}. The proposed biosensor will extend the application of nanomaterials in ECL immunoassays and open a new road for the detection of Brom and other β-AA in the future.

1. Introduction

β-adrenergic agonists (β-AA) with perfect nutrition redistribution function have been used for the livestock industry such as ruminants and pigs to reduce adipose tissue accretion and increase muscle mass while enhancement of feed conversion and growth rate [1–3]. β-AA with stable properties can be easily deposited in human body after meat consumption, which triggered off the symptoms of serious health problems such as muscular pain, dizziness cardiac and palpitation [4]. Although the EU and China have listed the β-AA as directory of prohibited drugs for animals feed, β-AA was still used as feed additives by some unscrupulous businessmen for economic interests [5]. In order to elude the official controls, a number of new compounds have been developed from β-AA such as Brombuterol (Brom). Brom (4-amino-3,5-dibromo-α[(tert.-butyl-amino) methyl] benzyl alcohol) is certainly known a representative of the class of aryl amine β-AA [6]. Brom have received extensive attention for their illegally used, however, only few studies specialized on Brom were in the scientific literature. Therefore the effective means for detecting Brom or other β-AA residues in food and feed are badly in need of improvement.

Presently, various analytical methods of β-AA and related compounds have been developed in an effort to combat the illegal usage. These methods include high performance liquid chromatography (HPLC) [7], ultra-high performance liquid chromatography hyphenated to tandem mass spectrometry (UHPLC/MS/MS) [8], a liquid chromatography-mass spectrometry (LC-MS) [9,10], enzyme-linked immunosorbent assay (ELISA) [6,11], gas chromatography-mass (GC-MS) [6], etc. There are some disadvantages of the above methods, such as sample treatment for a long time, cumbersome detection process and difficult to operate, expensive instruments and phenomenon of false positives, which limit their practical applications. In this paper, electrochemiluminescent immunoassay (ECLIA) prepared by competition immune as an effective method has been used for detecting Brom.

ECL involved the generation of species via electron red-ox processes of substance on the surfaces of electrode, undergone electron-transfer reactions to form excited states and then caused emission of light [12,13]. Since the first putforward ECL studies, the ECL with many distinct characteristics (such as no radioisotopes useing, temporal and spatial controlling, rapid measurement and far low detection limits of label) has attracted much interest [14–16]. ECLIA as a powerful bioanalysis technique is composed of ECL and immunoassay with values of specific identification, stability, simplified optical setup, high sensitivity, wide dynamic range and weak background signal [13]. The ECLIA methods developed mainly on two mechanisms: consumption of ECL coreactant in reaction and steric hindrance produced from the formation of immunocomplex [17]. In this experiment, consumption of CdSe QD based immunosense (ECL coreactant) resulted from an immune reaction, which could be generated by changing the combination of the CdSe QDs-labeled antibody and coating antigen (Ag-OVA) through varying Brom standard solution.

In recent years, there are some novel labeling agents (semiconductor nanocrystals [18], metallic oxide semiconductors [19] and carbon nanocrystals [20], etc.) and immobilization support (grapheme [21], carbon nanotubes [22], ZnO nanotube arrays [23], etc.) for ECL immunosensors. Moreover, low toxic CdSe QDs for eco-friendly alternatives QD-ECL probes with great interest was prepared in aqueous phase L-cysteine as the stabilizer [24]. L-cysteine can avoid the aggregation of quantum dots, as well as it possesses a favorable biocompatibility, which would be as a good ECL luminophore for further extending the analytical performance of CdSe QD-based ECL biosensors.

According to its particularity properties of nanomaterials and some unique physicochemical property in catalytic chemistry, electronics, energy and biological fields, noble metal nanomaterial act as an important part of metal nanomaterial had widely application prospects and caused more and more attention of scientists. Gold and silver nanomaterials with abundant electrical and optical properties, good stability and low biological toxicity also have attributed widespread concern in the fields of physics, chemistry, materials, etc [25–28]. Due to their stability, high specific surface area, and biocompatibility, AuNPs have attracted tremendous attention in the area of applications like catalysis and bioanalysis [29]. In this work, AuNPs with negatively charged in weakly alkaline conditions can be combined with positive charge on the protein molecule groups by means of the electrostatic interactions, which do not affect the biological activity of the protein. Polyamidoamine dendrimers (PAMAM) with high geometric symmetry, precise molecular structure, a large number of functional groups, good biocompatibility, molecular memory in the cavity and the molecular chain growth controlled properties has attracted extensive attention in sensor fields. Since the amino groups possessed a high reaction activity and easily modified could be employed to bond abundant actived QDs to further amplify ECL signal. We synthesized silver-cysteine hybrid nanoribbon (SNR) by a simple and green one-step aqueous chemical synthetic strategy [30,31]. Firstly, the prepared SNR are monodispersed nanoribbon with diameter of 500 nm and length of 3 μm, have abundant carboxyl groups (-COOH) on their surfaces and fabricate amplified SNR-PAMAM-QDs ECL signal probe [32]. We have put forward a SNR amplified QDs competitive immunoassay for sensitive detection of Brom for the first time. Then, AuNPs were decorated on the surface of the SNR-PAMAM via Au-N bonds [33]. The formed AuNPs-PAMAM-SNR composite possessed larger specific surface area, which could effectively immobilize the abundant Ag-OVA to enhance the ECL signal. On one hand, SNR avoided the aggregation of AuNPs on electrode, and on the other hand, the excellent electric conductivity made AuNPs-PAMAM-SNR on the surface of GCE act as good accelerators for improving the electrochemical reaction efficiency of QDs and $K_2S_2O_8$. Therefore, PAMAM (16 -NH_2) functionalized SNR (SNR-PAMAM) with numerous amino groups would exhibit potential applications in immunosensors.

Herein, taking advantages of AuNPs, SNR-PAMAM and biocompatibility of CdSe QDs, we design a new multiple amplified ECL immunosensor, where Brom is detected as target, the SNR-PAMAM-AuNPs-Ag-OVA as substrate and Brom-Ab-SNR-PAMAM-CdSe QDs act as the ECL signal probes. The standard solutions of Brom compete with quantitative Brom Ag-OVA for limited specific binding sites of the Brom-Ab-SNR-PAMAM-CdSe QDs to form an immunocomplex. When Brom increased, the obtained Brom-Ab-SNR-PAMAM-CdSe QDs with competition bounding to the electrode surface was reduced, which result ECL signal decreased.

Hence, ECL intensity mainly depended on the quantity of Brom and was with a certain linear relationship of the concentration of Brom. In this work, we employed SNR modified AuNPs (SNR-AuNPs) as substate instead of simple AuNPs, which avoid agglomerating and denaturizing of AuNPs. Moreover, we prepared the ECL probe by using the total different materials such as SNR and PAMAM. The success of the synthesis of the probe provided more active sites for antibody loading and multiple amplified the ECL intensity. Compared with some previous literature [34,35], we could obviously find that the ECL intensity changed significantly with per unit concentration of Brom, thus this immunosensor possessed higher sensitivity. In general, we have established a brand new biosensor with novel material and especial electrode assembly process which possessed higher sensitivity for detecting small molecule. Based on this theory, a novel and ultrasensitive competitive immunosensor showed a new promising platform for detecting Brom or other β-AA.

2. Materials and methods

2.1. Reagents and apparatus

Cadmium chloride ($CdCl_2 \cdot 2.5H_2O$, 99%), ethyl alcohol (99.7%), Se powder (99.95%), sodium borohydride ($NaBH_4$, 96%), monopotassium phosphate (KH_2PO_4, 99%), disodium hydrogen phosphate dodecahydrate ($Na_2HPO_4 \cdot 12H_2O$, 99%), potassium chloride (KCl, 99.5%), chloroauric acid ($HAuCl_4 \cdot 4H_2O$, 47.8%), trisodium citrate (99%), potassium peroxodisulfate ($K_2S_2O_8$, 99.5%), L-cyseine hydrochloride monohydrate (L-cysteine), Bovine serum albumin (BSA, 98%), Ethyl-3-(dimethyl aminopropyl) carbodiimide (EDC, 98%) and N-hydroxysuccinimide (NHS, 97%) were purchased from Sinopharm Chemical Reagent Co., Ltd (Shanghai, China). Silver nitrate($AgNO_3$) was purchased from Jiangsu Qiangsheng Chemical Co., Ltd. Polyamidoamine dendrimers (PAMAM, G2) were purchased from Weihai CY Dendrimer Technology Co., Ltd. Salbutamol (SAL), brombuterol (Brom), clenbuterol (CLB), ractopamine (RAC) and phenylethanolamine A (PA) were obtained from National Institutes for Food and Drug Control (Beijing, China). Phosphate buffered saline (PBS) prepared by $Na_2HPO_4 \cdot 12H_2O$, KH_2PO_4 and NaCl was used throughout the whole work. All other reagents and chemicals were commercially available and of analytical reagent grade. All aqueous solutions were prepared with sub-boiling doubly distilled water.

2.2. Apparatus

The electrochemical measurement for ECL was carried out on a MPI-A multifunctional electrochemical and chemiluminescent analytical system (Xi'An Remax Electronic Science & Technology Co., Ltd, Xi an, China). The experiment applied a conventional three-electrode system with a modified glassy carbon electrode (GCE, 3 mm diameter) as working, a platinum wire as auxiliary, and an Ag/AgCl (saturated KCl solution) as reference electrodes. Cathodic potential in a range from 0 to −1.6 V was applied to the GCE electrode using the cyclic voltammetric (CV) technique, while the ECL emission was recorded. The photomultiplier tube (detection range from 300 to 800 nm) was biased at −650 V. UV–vis absorption spectra were recorded with Agilent 8453 UV–vis photospectrometer (Agilent Co., USA). The High Resolution Transmission Electron Microscope (HRTEM) images were obtained from Tecnai G2 F20 S-TWIN 200 KV (FEG, FEI Co., USA). The dynamic light scattering (Dls) and zeta potential was taken on a Malvern Zetasizer Nano ZS 90 (UK). Electrochemical impedance spectroscopy (EIS) images were carried out with a RST electrochemical working station (Suzhou Risetest Instrument Co., Ltd, China), using the same three-electrode system as that in the ECL detection.

2.3. Preparation of the Brom coating antigen and Brom antibody

The preparation of Brom coating antigen and antibody were according to our previous literature [11,36]. In brief, 2.8 mg brombuterol were dissolved in 300 μL distilled water, and 2.4 mg $NaNO_2$ were injected dropwise under slowly stirring, and then adjusted pH to 1.5 with 0.2 M HCl. The reaction was placed in the dark for 7 h at 4 °C and the solution was from colorless to bright yellow. In the diazotize solution, after primary testing with N, N′-dimethylaniline, and the reaction was stopped by addition of 5.5 mg carbamide solution. On the basis of carbamide excess: excess carbamide would change the starch iodide paper into blue. The above diazotized brombuterol was added dropwise with a solution of protein (44.5 mg BSA or 33 mg OVA) in 1.5 mL of PBS, and was adjusted to pH 7.5 by adding a small amount of 1 M NaOH. The reaction was continued under slightly stirring overnight at 4 °C. The solution was intensively dialyzed in 0.01 M PBS for 5 days with several changes of the dialyzing buffer solution, lyophilized, and stored at −20 °C until use. Then the Brom-OVA were selected as coating antigen, while the Brom-BSA was used as immunogen for antibody production.

After that, polyclonal antibodies against Brom were obtained from antisera of white New Zealand rabbits. After 5 times immunization, the serum was dissolved out, the blood was centrifugated and obtained supernatant. Then the supernatant was blended with isopyknic normal saline (NS), and saturated ammonium sulfate solution was added to the mixture to precipitate protein for three times. The precipitate was obtained by centrifugation and dissolved in NS. Polyclonal antibodies against Brom was obtained and stored at −40 °C before use. The above animal experiments have been approved by the institutional committees, and were performed in compliance with the relevant laws and institutional guidelines.

2.4. Synthesis of silver nanoribbon

Silver nanoribbon (SNR) was synthesized according to the literature [30]. 88 mg $AgNO_3$ and 121 mg L-cyseine were dissolved with 10 mL distilled water. The prepared strong acid muddy solution was adjusted pH to 9.0 with NaOH under vigorously stirring, and then germinated for 24 h at room temperature (RT). White precipitates were obtained and further centrifugalize (6000 rpm). The precipitation was washed with distilled water to neutral, and then dried under vacuum at 60 °C. SNR was acquired and stabled for 6 months at RT.

2.5. Preparation of probe

The preparation of water-soluble L-cysteine-capped CdSe QDs was referred to our previous reported method [24]. Firstly, 200 μL CdSe QDs were mixed with 200 μL ethyl alcohol solutions to concentrate by centrifuging (10000 rpm, 5 min). Then, 20 μL 200 μg mL^{-1} EDC and 20 μL 200 μg mL^{-1} NHS were added to activate the carboxyl group of quantum dots under stirring for 2 h. Next, 10 μL PAMAM (1 mg mL^{-1}) solutions were added to 10 μL SNR and reacted for 2 h. Excess reagents were removed by subsequent centrifugation and redispersion in water. Activated CdSe QDs was connected to the SNR by dehydration condensation reaction between amino group and carboxyl group (seen from Scheme 2A). 10 μL Brom antibodies (Ab) solution were dropped in the acquired SNR-PAMAM-CdSe QDs composite solution, and the solution was placed in the refrigerator for overnight. At next day, 10 μL 5% BSA was added for hatching 1 h to enclose nonspecific binding sites. Through the centrifugal remove excess reagent in the solution. The probe (Brom-Ab-SNR-PAMAM-CdSe QDs solution) was obtained for using (Scheme 1.1).

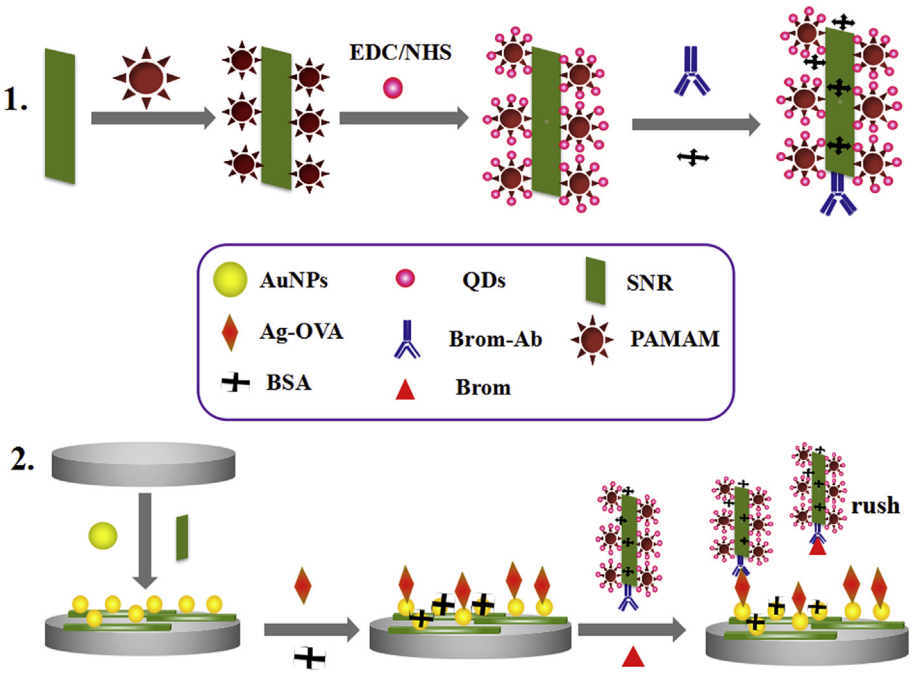

Scheme 1. (1) Preparation of Brom-Ab-SNR-PAMAM-CdSe QDs probe; (2) Fabrication of the GCE/SNR-PAMAM/AuNPS/Ag-OVA immunosensor.

2.6. Fabrication of the immunosensor

The fabrication process of the ECL immunosensor was schematized in Scheme 1.2. In the first place, 5 μL of PAMAM-SNR (0.01 mg mL^{-1}) and 10 μL concentrated AuNPs were successively dropped on the cleaned glassy carbon electrode (GCE) and evaporate at RT to form a stable film. Therein, SNR was on the electrode surface through connection of electrostatic adsorption. AuNPs connected to PAMAM-SNR by bonding of Au-N. Then, Brom Ag-OVA was dropped on a modified GCE for overnight at 4 °C. Similarly, Ag-OVA connect to AuNPs also by bonding of Au-N. 10 μL BSA was added for 1 h to block the excessive nonspecific binding sites.

2.7. Detection of the immunosensor

First of all, 10 μL different concentrations standard solution of Brom and signal probes mingled to obtain a hatching solution. Then, the hatching solution was immersed in the resultant GCE for 1 h. After the prepared GCE was washed with PBS (0.01 M, pH 7.4), the ECL measurement was performed in PBS (0.1 M, pH 7.4) containing of 0.1 M $K_2S_2O_8$ and 0.1 M KCl. ECL signal was produced by the electron energy transfer between the QDs and the $S_2O_8^{2-}$ (Scheme 2C). The ECL intensity of the immunosensor would decrease with the increasing concentration of the Brom in the detection solution, which was attributed to the competitive immunoassay between the Brom in incubation solution and the immobilized Ag-OVA for the limited binding sites of the Ab (Scheme 2B, curve a, b). Therefore, there was a correlative linear relationship between ECL intensity and Brom standard solution, which can be used as the quantitative criterion of Brom.

3. Results and discussion

3.1. Characterization of L-cysteine-capped CdSe QDs, SNR and SNR-PAMAM-CdSe QDs

Fig. 1 shows the surface morphologies and characterization of different nanomaterials using TEM, SEM and zeta potential. Fig. 1A showed the TEM of L-cysteine-capped CdSe QDs possessed homogeneous pherical particles with the size about 4 nm. Fig. 1B showed the SEM image of the SNR, which exhibited lengths of all samples were ranged from 2 to 4 μm and the diameter were from 300 to 600 nm. Hence, the SNR with huge specific surface area and binding sites could be used as perfect amplifying framework to assemble CdSe QDs, and showed promising potential for ECL immunoassay. CdSe QDs were loaded on the SNR by means of PAMAM to develop amplified SNR-PAMAM-CdSe QDs ECL signal probe. The SEM of SNR-PAMAM-QDs (Fig. 1C) could be seen that surface of SNR was quite rough, which indicated abundant QDs were connected to SNR. In addition, by comparing the inset of Fig. 1B and C, smooth surface of SNR was over covered with QDs. Fig. 1D shows zeta potential of (a) SNR, (b) SNR-PAMAM and (c) SNR-PAMAM-QDs. Due to the surface connected with a large number of positive charged amino group of PAMAM, zeta potential of SNR-PAMAM was apparently more positive than potential of pure SNR. When the surface loaded with QDs, absolute value of zeta potential reduced with the enhancement of intermolecular cohesion. In conclusion, these results demonstrated the successful preparation of the material.

3.2. Characterization of AuNPs

As shown the TEM in Fig. 2A, the actual size of AuNPs was about 20 ± 0.5 nm, which could provide more electroactive binding sites for the immobilization of Ag-OVA. In addition, the distribution of the AuNPs were tested by DLs. As shown in Fig. 2B, the sizes of AuNPs distribute from 11 nm to 35 nm and the average grain size is 19.16 nm. Herein, the AuNPs have uniform size distribution and good dispersion.

3.3. ECL mechanism of immunosensor

To study the effect of $S_2O_8^{2-}$ as co-reaction accelerator on the ECL reaction process, we also compared the CV curves of GCE with probe containing CdSe QDs (Fig. 3A), $K_2S_2O_8$ (Fig. 3B) and CdSe QDs/

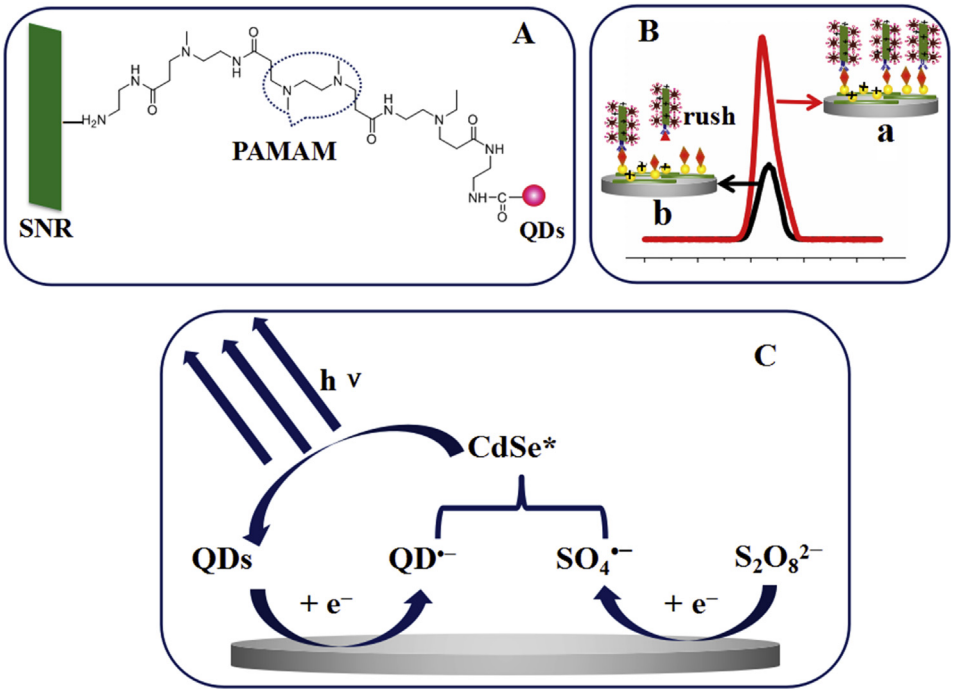

Scheme 2. (A) The bonding illustration of SNR-PAMAM-CdSe QDs; (B) The comparison of ECL intensity between without Brom (curve a) and with Brom (curve b); (C) Illustrative ECL reaction mechanism of the immunosensor.

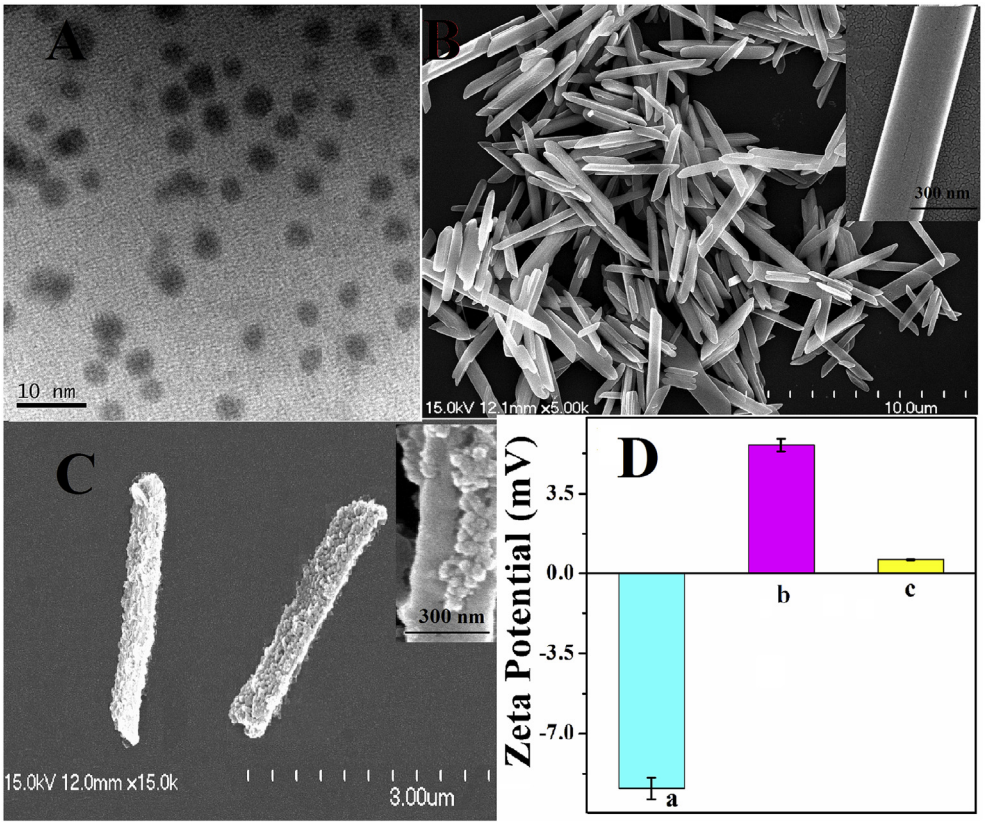

Fig. 1. (A) HRTEM image of L-cysteine-capped CdSe QDs, (B) SEM image of SNR, (C) SEM image of SNR-PAMAM-CdSe QDs and (D) zeta potential of SNR (a), SNR-PAMAM (b) and SNR-PAMAM-QDs (c).

$K_2S_2O_8$ (our immunosensor, Fig. 3C) (where the working potentials were both set at the 0 ~ −1.6V). As shown in Fig. 3A, an reduction peaks in the voltage of −1.28 V could be observed in the solution of PBS with probe and without $K_2S_2O_8$, which indicated that this peak (−1.28 V) could be attributed to the reduction of the CdSe QDs. Similarly, Fig. 3B confirmed the reduction peak of $S_2O_8^{2-}$ at −0.65V

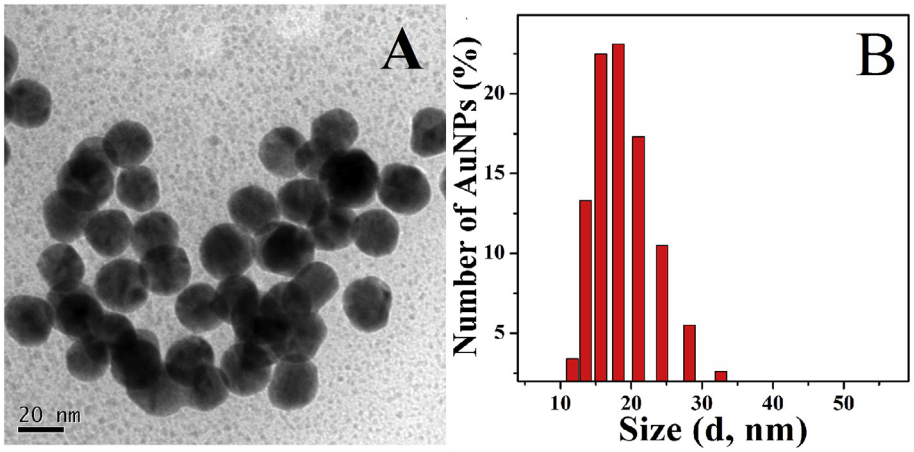

Fig. 2. HRTEM image (A) and DLs (B) of AuNPs.

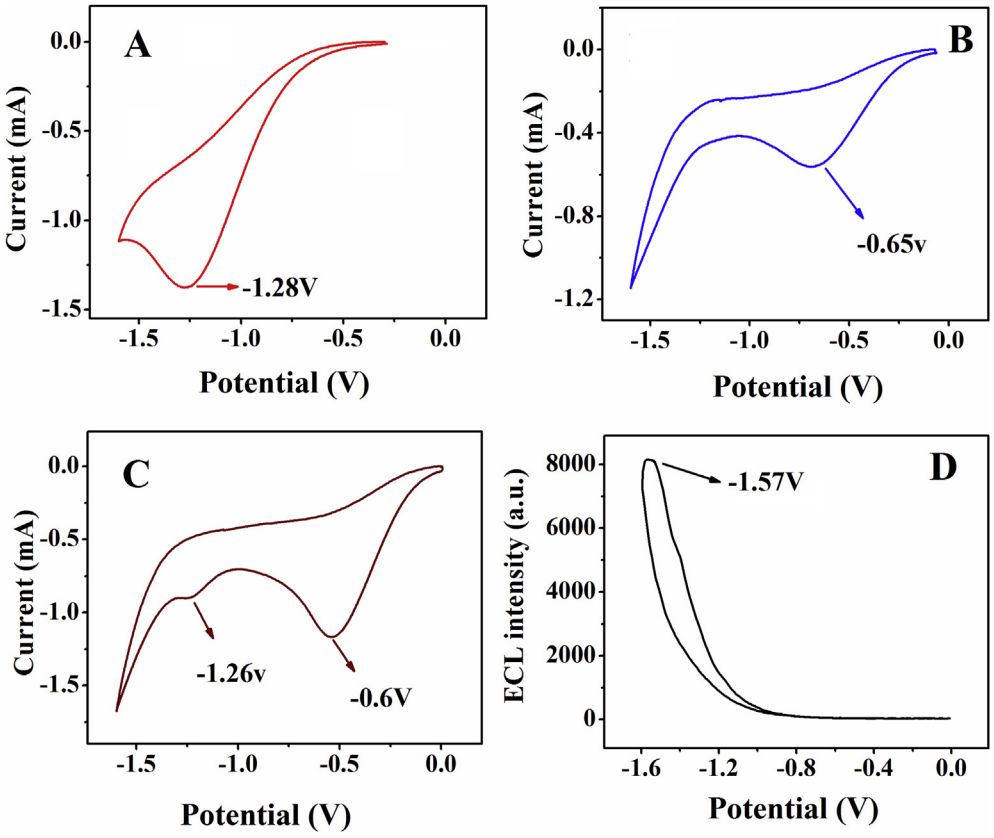

Fig. 3. (A) Cyclic voltammogram of immunosensor (A) with probe containing CdSe QDs without $K_2S_2O_8$, (B) with $K_2S_2O_8$ without probe and (C) with probe and $K_2S_2O_8$ in 0.1 M PBS (pH 7.4). (D) Cyclic voltammogram of immunosensor in 0.1 M PBS containing 0.1 M $K_2S_2O_8$. Scan rate: 100 mV s^{-1}.

in the PBS containing of $K_2S_2O_8$ without probe. When the GCE was measured in CdSe QDs/$K_2S_2O_8$ solution, Fig. 3C showed that two reduction peaks of CdSe QDs and $S_2O_8^{2-}$ were appeared at −1.26 V and −0.6 V, respectively. There were a slight shifted of potential compared with pure CdSe QDs and $K_2S_2O_8$ solution, owing to the interaction between CdSe QDs and $S_2O_8^{2-}$. When the potential was negative at −1.26 V, CdSe obtain an electron to be electronegative $CdSe^{\bullet-}$ (Eq. (1)). Meanwhile, the potential was at −0.6 V, negatively charged radicals $SO_4^{\bullet-}$ and SO_4^{2-} was resulted from the reduction of $S_2O_8^{2-}$ (Eq. (2)). Then, the excited state of CdSe* could be generated by the radical annihilation reaction between the strong oxidant $SO_4^{\bullet-}$ and $CdSe^{\bullet-}$, according to injecting a hole into the highest occupied molecular orbital of $CdSe^{\bullet-}$ (Eq. (3)). Furthermore, a small amount of dissolved oxygen in the solution will also get electron to generate OOH^- (Eq. (4)). OOH^- as a co-reaction agent reacted with negatively charged $CdSe^{\bullet-}$ to form CdSe* (Eq. (5)). However, unstable excited states of CdSe* would back to ground state and accompanied with strong electrochemical luminescence signal (Eq. (6)). An intensive ECL emission peak could be observed about at −1.57 V (Fig. 3D). In short, combined with the above discussion and previous literature reports [37–39], the possible mechanism was inferred as follows:

$$CdSe + e^- \rightarrow CdSe^{\cdot -} \quad (1)$$

$$S_2O_8^{2-} + e^- \rightarrow SO_4^{2-} + SO_4^{\cdot -} \quad (2)$$

$$SO_4^{\cdot -} + CdSe^{\cdot -} \rightarrow CdSe^* + SO_4^{2-} \quad (3)$$

$$O_2 + H_2O + 2e^- \rightarrow OOH^- + OH^- \quad (4)$$

$$2CdSe^{\cdot -} + OOH^- + H_2O \rightarrow 3OH^- + 2CdSe^* \quad (5)$$

$$CdSe^* \rightarrow CdSe + h\nu \quad (6)$$

3.4. ECL characterization of stepwise fabrication and signal amplification

EIS as a parameter is applied to characterize the interface properties of surface-modified electrode [40,41]. Hence, the stepwise assembly of immunosensor was studied by EIS in 0.1 M KCl containing 5 mM $[Fe(CN)_6]^{3-/4-}$. In the EIS Nyquist plots, the semicircle portion diameter corresponds to the electron-transfer resistance (Ret). As shown in Fig. 4A, the bare GCE exhibited a very small Ret (curve a). When the bare GCE was incubated with SNR (curve b), the Ret of the GCE gradually increased, which is due to the steric hindrance of micrometer size of SNR. Owing to the excellent electrical conductivity of AuNPs, the Ret of GCE/SNR/AuNPs (curve c) become much lower than GCE/SNR. Subsequently, with the step-by-step immobilization of Ag-OVA and BSA on the electrode, the Ret greatly increased (curve d and curve e) because of the protein layer generated a barrier for electron-transfer. Hence, EIS results confirm that the ECL immunosensor was successfully fabricated with different modification steps.

In addition, the stepwise fabrication process of the biosensor was characterized by cyclic voltammetry (CV) measurements in the presence of 0.1 M KCl containing 5 mM $[Fe(CN)_6]^{3-/4-}$. The redox peak current of GCE/SNR (curve b) decreased remarkably compared with bare GCE (curve a), since SNR on the electrode as micron scale size with the area steric hindrance. When AuNPs were coated on the electrode surface (curve c) compared with bare GCE/SNR (curve b), the current obviously increased which attributed to the conductivity of AuNPs accelerated the electron transfer. Nevertheless, the current decreased consecutively after the successively immobilization of Ag-OVA, BSA (curves d and e) on account of the formation of protein molecules layers obstructed the electron transfer.

As shown in Fig. 4C, the ECL characterizations of the fabrication process of the immunosensor with bare GCE (curve a), GCE/SNR/AuNPs/Ag-OVA (curve b), GCE/SNR/AuNPs/Ag-OVA/Ab-QDs (curve c) and GCE/SNR/AuNPs/Ag-OVA/Ab-SNR-PAMAM-QDs (curve d) were performed in PBS (0.1 M, pH 7.4) containing of 0.1 M $K_2S_2O_8$ and 0.1 M KCl. A low ECL response was observed from the bare GCE (curve a). When SNR/AuNPs/Ag-OVA composite was coated on the electrode, the ECL intensity was enhanced (curve b), because AuNPs accelerate the electron transfer in the surface of GCE. After signal probe with SNR were dropped on electrode surface, the ECL signal (curves d) was exhibited apparently higher than the probe without SNR (curve c). SNR enriched a large number of QDs via PAMAM, which played an important role in amplification of the ECL signal.

3.5. Optimization of experimental conditions

In order to maximize the immunosensor response, the experimental conditions including concentration of Ab, Ag-OVA and the amount of SNR on the surface of GCE were investigated. Therein, the ΔECL was the difference between the ECL responses of immunosensor for Brom detection at 0 and 1000 ng mL^{-1}. Fig. 5A showed that ΔECL enhanced with the increasing concentration of Ab from 2 to 16 μg mL^{-1}, which contributed to the increasing of the quantity of signal probe conjugated on the surface of the electrode. Due to the saturation of the electrode surface area, the ΔECL slowly increased and tended to level off with the concentration beyond 16 μg mL^{-1}. Therefore, 16 μg mL^{-1} was chosen as the optimal Ab concentration. Similarly, 25 μg mL^{-1} Ag-OVA was selected for subsequent experiments (Fig. 5B). Furthermore, when the volume of SNR on the surface of GCE (C_{SNR} = 0.01 mg mL^{-1}) increased from 2 to 6 μL, the ΔECL enhanced and showed the maximum value at 6 μL with the active SNR accelerating the electron transfer and preventing condensation of AuNPs (Fig. 5C). Then, with a further increase of the volume from 6 to 10 μL of SNR, according to steric hindrance of SNR, the ECL quenching turned down. So the optimal volume of SNR was selected as 6 μL.

3.6. Detection, selectivity, stability and reproducibility of the ECL immunosensor

Under the above optimized conditions, the ECL response of the immunosensor towards different concentration Brom were detected in PBS (0.1 M, pH 7.4) containing of 0.1 M $K_2S_2O_8$ and 0.1 M KCl. As seen from Fig. 6A, the ECL intensity increased linearly with the

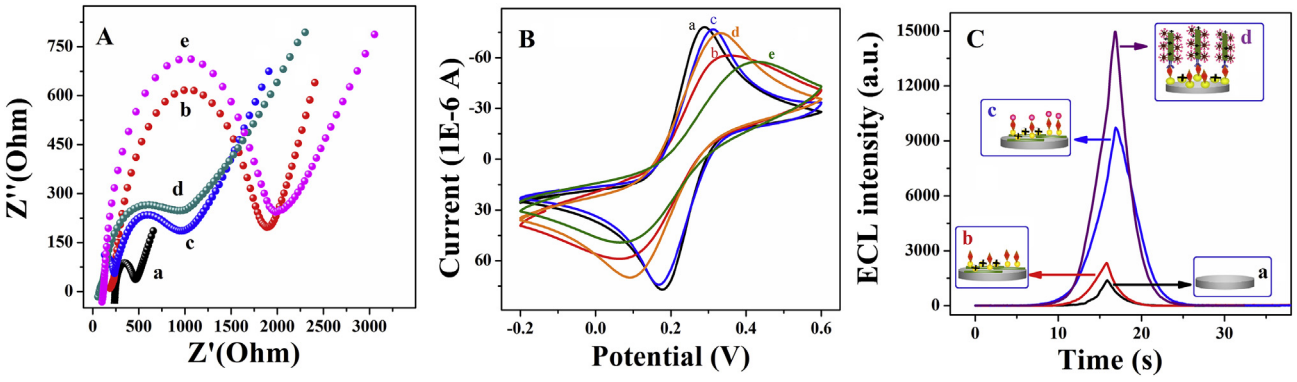

Fig. 4. (A) Electrochemical Impedance Spectroscopy and (B) Cyclic voltammogram of (a) bare glassy carbon electrode (GCE), (b) GCE/SNR, (c) GCE/SNR/AuNPs, (d) GCE/SNR/AuNPs/Ag-OVA and (e) GCE/SNR/AuNPs/Ag-OVA/BSA in 0.1 M PBS containing 2.5 mM $[Fe(CN)_6]^{3-}$/$[Fe(CN)6]^{4-}$ and 0.1 M KCl. (C) ECL intensity of the fabrication process of the immunosensor with bare GCE (curve a), GCE/SNR/AuNPs/Ag-OVA (curve b), GCE/SNR/AuNPs/Ag-OVA/Ab-QDs (curve c) and GCE/SNR/AuNPs/Ag-OVA/Ab-SNR-PAMAM-QDs (curve d) were performed in 0.1 M PBS containing of 0.1 M $K_2S_2O_8$.

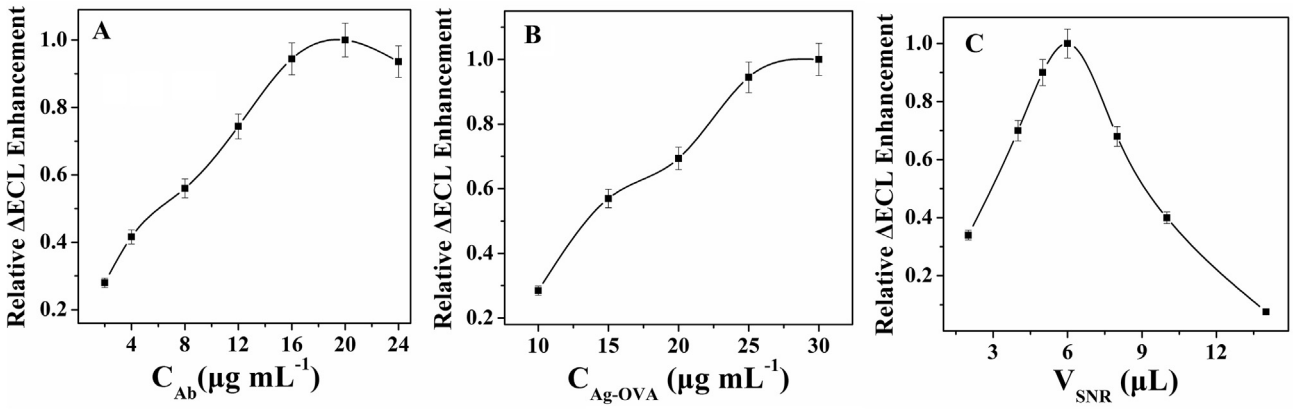

Fig. 5. Optimization of (A) concentration of Brom Ab, (B) concentration of Brom Ag-OVA and (C) the volume of SNR on the surface of GCE for immunoreaction conditions. The ECL emission was detected in 0.1 M PBS containing 0.1 M $K_2S_2O_8$.

increase of Brom concentration in the range of 0.005–700 ng mL^{-1}. The calibration curve was presented in Fig. 6B and the linear regression equation was Y = 7887.42–1986.11 log [Brom] (ng mL^{-1}) (R^2 = 0.9934) with detection limit (S/N = 3) of 1.5 pg mL^{-1}. Therefore, the proposed biosensor possessed a higher sensitivity and wider dynamic response range for detection of Brom.

The ECL biosensor possessed good specificity for Brom was evaluated by challenging the immunosensor toward other common interferents of CLB, SAL, RAC and PA at 10 ng mL^{-1} and 100 ng mL^{-1}, respectively. From Fig. 6C, SAL, RAC and PA did not cause the interference in the test of our biosensor. Due to their very similar molecule structures [42], however, the cross-reactivity of Brom with CLB was 8.47% (10 ng mL^{-1}) and 11.78% (100 ng mL^{-1}). It was demonstrated that this immunosensor exhibited a high selectivity and an acceptable specificity for the detection of Brom. The stability and reproducibility of the biosensor were also evaluated in Fig. 6D. Under the successive scanning 7 cycles for the detection of Brom with the concentration of 0.5, 5 and 50 ng mL^{-1}, the RSD were from 0.83% to 1.55%, which revealing that the immunosensor possessed an acceptable stability for Brom detection.

3.7. Application to actual samples

The practical application feasibility was analyzed by detecting pork and feed (randomly collected from the market in Suzhou). The pretreatment process of pork and feed samples were consistently

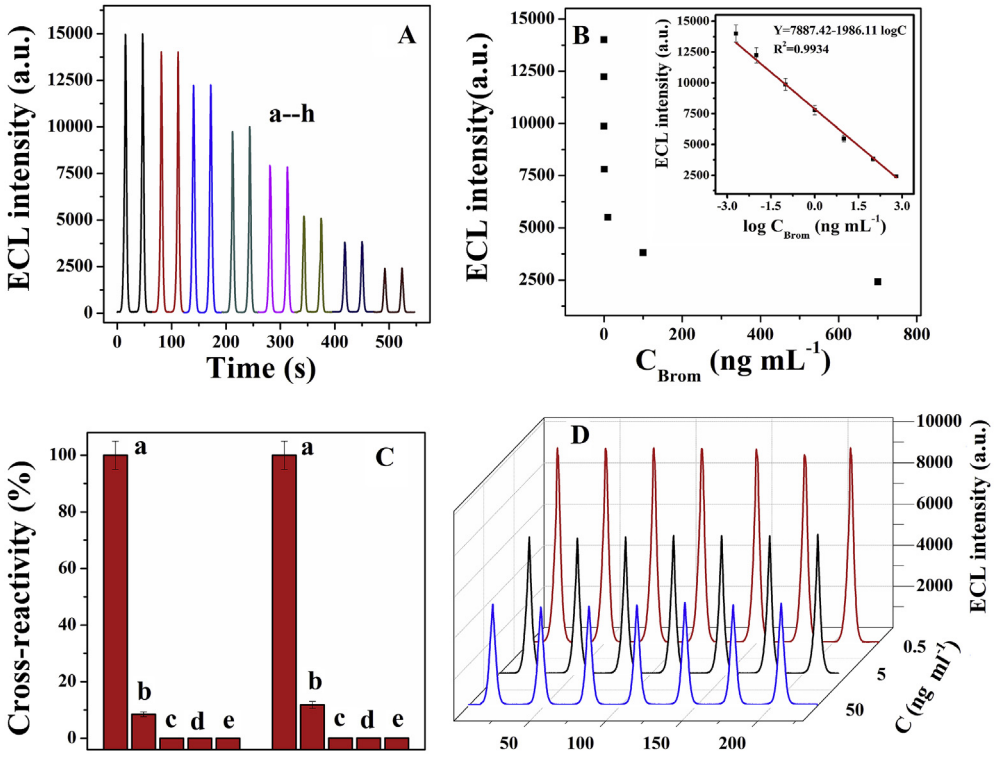

Fig. 6. (A) ECL curves of immunosensor for Brom detected at (a) 0, (b) 0.005, (c) 0.015, (d) 0.1, (e) 1, (f) 10, (g) 100 and (h) 700 ng mL^{-1}. (B) Linear calibration curve of the immunosensor in different Brom concentration from 0.005 to 700 ng mL^{-1}. (C) Selectivity of the developed immunosensor for Brom (a) detection over CLB (b), SAL (c), RAC (d) and PA (e) at concentration of 10 ng mL^{-1} and 100 ng mL^{-1}, respectively. (D) Continuous cyclic scans of immunosensor for 7 cycles formed at 0.5, 5 and 50 ng mL^{-1} Brom standard solutions in 0.1 M PBS containing 0.1 M $K_2S_2O_8$.

Table 1
Recovery tests of Brom spiked in the actual samples by the proposed method (n = 3).

Sample types	Add (ng mL^{-1})	Found (ng mL^{-1})	Intra-assay RSD (%)	Recovery (%)
Pork sample 1	0	N. D.[a]	–	–
Pork sample 2	0.05	0.052 ± 0.001	2.25%	103%
Pork sample 3	5	5.45 ± 0.18	3.62%	109%
Pork sample 4	50	55.1 ± 0.97	1.94%	110%
Feed sample 1	0	N. D.	–	–
Feed sample 2	0.05	0.049 ± 0.0005	1.05%	98.6%
Feed sample 3	5	5.74 ± 0.031	0.62%	115%
Feed sample 4	50	54.25 ± 2.83	5.67%	108%

[a] N.D. = not detected.

as our previous literature [43]. The prepared samples were detected by replacing Brom standard samples and were no Brom residuals detected in the actual samples (Table 1). Hence, they could be used as blank samples. Three concentrations of Brom (0.05, 5, and 50 ng mL^{-1}) were measured by our biosensor with recoveries from 98.6% to 115% and the intra-assay RSD from 0.62% to 5.67%, respectively. All these results confirmed the satisfactory accuracy and reliability of the proposed immunosensor in actual samples.

4. Conclusions

In summary, a novel and highly sensitive ECL immunosensor has been proposed for the determination of Brom based on GCE/SNR-PAMAM/AuNPS/Ag-OVA/Ab-SNR-PAMAM-QDs. L-cysteine capped CdSe QDs with high stability was prepared by using low-cost and green materials, and were very suitable for ECL sensing and detection. AuNPs not only promoted the electrode transfer between QDs and the electrode but also possessed large electroactive surface to enhance the loading capacity of the Ag-OVA combining with more CdSe QDs labeled Brom antibody, which have been provide signal amplification for ECL intensity. SNR-PAMAM-AuNPs on the surface of electrode can be act as good accelerators for electron transfer. In addition, PAMAM functionalized SNR as probe with numerous amino groups could be employed to bond abundant actived QDs to further amplify ECL signal. Hence, through multi-step amplification effect, the multiple amplification immunosensor was frabricated. We also have confirmed that the ECL immunosensor exhibited good sensitivity, reproducibility and stability, which successfully provided a new strategy for determination of Brom. Hence, the perfect performance of the immunosensor would open a new way for β-AA determination in routine and practical analyses.

Acknowledgments

We gratefully acknowledge the Science Fund from the National Natural Science Foundation of China (No. 21075087, No. 21175097), the Project of Scientific and Technologic Infrastructure of Suzhou (SZS201207), and the Project Funded by the Priority Academic Program Development of Jiangsu Higher Education Institutions (No. YX10900212).

References

[1] J.J. Bradley, B.S. Stephen, Y.C. Ki, Historical overview of the effect of β-adrenergic agonists on beef cattle production, J. Anim. Sci. 27 (2014) 757–766.
[2] T.T. Li, J.J. Cao, Z. Li, X. Wang, P.L. He, Broad screening and identification of β-agonists in feed and animal body fluid and tissues using ultra-high performance liquid chromatography-quadrupole-orbitrap high resolution mass spectrometry combined with spectra library search, Food Chem. 192 (2016) 188–196.
[3] M.S. da S. Ferreira, C.A.P. Garbossa, G. Oberlender, L.J. Pereira, M.G. Zangeronimo, R.V. de Sousa, V. de S. Cantarelli, Effect of ractopamine on lipid metabolism in vivo - a systematic review, Arch. Biol. Technol. 56 (2013) 35–43.
[4] Y. Zhou, P.L. Wang, X.O. Su, H. Zhao, Y.J. He, Colorimetric detection of ractopamine and salbutamol using gold nanoparticles functionalized with melamine as a probe, Talanta 112 (2013) 20–25.
[5] T.S. Brand, M.P. Genis, L.C. Hoffman, W.F.J. van de Vyver, R. Swart, G.F. Jordaan, The effect of dietary energy and the inclusion of a β-adrenergic agonist in the diet on the meat quality of feedlot lambs, S. Afr. J. Anim. Sci. 43 (2013) S140–S145.
[6] E. Sangiorgi, M. Curatolo, Application of a sequential analytical procedure for the detection of the β-agonist brombuterol in bovine urine samples, J. Chromatogr. B 693 (1997) 468–478.
[7] A. Koole, J. Bosman, J.P. Franke, R.A. Zeeuw, Multiresidue analysis of β-agonists in human and calf urine using β_2 multimodal solid-phase extraction and high-performance liquid chromatography with electrochemical detection, J. Chromatogr. B 726 (1999) 149–156.
[8] D. Mauro, S. Ciardullo, C. Civitareale, M. Fiori, A.A. Pastorelli, P. Stacchini, G. Palleschi, Development and validation of a multi-residue method for determination of 18 β-agonists in bovine urine by UPLC–MS/MS, Microchem. J. 115 (2014) 70–77.
[9] P.R. Kootstra, C.J.P.F. Kuijpers, K.L. Wubs, D. van Doorn, S.S. Sterk, L.A. van Ginkel, R.W. Stephany, The analysis of beta-agonists in bovine muscle using molecular imprinted polymers with ion trap LCMS screening, Anal. Chim. Acta 529 (2005) 75–81.
[10] C. Juan, C. Igualada, F. Moragues, N. León, J. Mañes, Development and validation of a liquid chromatography tandem mass spectrometry method for the analysis of β-agonists in animal feed and drinking water, J. Chromatogr. A 1217 (2010) 6061–6068.
[11] H.J. Du, Y.X. Chu, H. Yang, K. Zhao, J.G. Li, P. She, X. Zhang, A.P. Deng, Sensitive and specific detection of a new β-agonist brombuterol in tissue and feed samples by a competitive polyclonal antibody based ELISA, Anal. Methods 8 (2016) 3578–3586.
[12] M.M. Richter, Electrochemiluminescence (ECL), Chem. Rev. 104 (2004) 3003–3036.
[13] S.Y. Deng, H.X. Ju, Electrogenerated chemiluminescence of nanomaterials for bioanalysis, Analyst 138 (2013) 43–61.
[14] K. Muzyka, Current trends in the development of the electrochemiluminescent immunosensors, Biosens. Bioelectron. 54 (2014) 393–407.
[15] S.E.K. Kirschbaum, A.J. Baeumner, A review of electrochemiluminescence (ECL) in and for microfluidic analytical devices, Anal. Bioanal. Chem. 407 (2015) 3911–3926.
[16] H. Mahdi, Z.F. Ding, Review-Electrogenerated chemiluminescence: light years ahead, J. Electrochem. Soc. 163 (4) (2016) H3116–H3131.
[17] J.P. Lei, H.X. Ju, Fundamentals and bioanalytical applications of functional quantum dots as electrogenerated emitters of chemiluminescence, Anal. Chem. 30 (2011) 1351–1359.
[18] W.W. Zhao, J. Wang, Y.C. Zhu, J.J. Xu, H.Y. Chen, Quantum dots: electrochemiluminescent and photoelectrochemical bioanalysis, Anal. Chem. 87 (2015) 9520–9531.
[19] C. Fu, Q. Xu, X.P. Wei, J.P. Li, Highly sensitive ECL immunosensor based on multi-labeling of luminol via a dendrimer on Fe_3O_4 Nanoparticles, RSC Adv. 4 (2014) 26102–26107.
[20] Y.H. Xu, J.Q. Liu, C.L. Gao, E.K. Wang, Applications of carbon quantum dots in electrochemiluminescence: a mini review, Electrochem. Commun. 48 (2014) 151–154.
[21] Y.H. Sha, Z.Y. Guo, B.B. Chen, S. Wang, G.P. Ge, B. Qiu, X.H. Jiang, A one-step electrochemiluminescence immunosensor preparation for ultrasensitive detection of carbohydrate antigen 19-9 based on multi-functionalized graphene oxide, Biosens. Bioelectron. 66 (2015) 468–473.
[22] H. Dai, G.F. Xu, S.P. Zhang, L.S. Gong, X.H. Li, C.P. Yang, Y.Y. Lin, J.H. Chen, G.N. Chen, Carbon nanotubes functionalized electrospun nanofibers formed 3D electrode enables highly strong ECL of peroxydisulfate and its application in immunoassay, Biosens. Bioelectron. 61 (2014) 575–578.
[23] W.J. Wang, Q. Hao, W. Wang, L. Bao, J.P. Lei, Q.B. Wang, H.X. Ju, Quantum dot-functionalized porous ZnO nanosheets as a visible light induced photoelectrochemical platform for DNA detection, Nanoscale 6 (2014) 2710–2717.
[24] X. Yao, P.P. Yan, Q.H. Tang, A.P. Deng, J.G. Li, Quantum dots based electrochemiluminescent immunosensor by coupling enzymatic amplification for ultrasensitive detection of clenbuterol, Anal. Chim. Acta 798 (2013) 82–88.

[25] L.L. Liu, Q. Ma, Y. Li, Z.P. Liu, X.G. Su, A novel signal-off electrochemiluminescence biosensor for the determination of glucose based on double nanoparticles, Biosens. Bioelectron. 63 (2015) 519–524.
[26] X. Ou, C. Fang, Y. Fan, H.M. Chen, S.H. Chen, S.P. Wei, Sandwich-configuration electrochemiluminescence biosensor based on Ag nanocubes-polyamidoamine dendrimer-luminol nanocomposite for Con A detection, Sens. Actuators, B 228 (2016) 625–633.
[27] M.N. Ma, Y. Zhou, R. Yuan, Y.Q. Chai, New signal amplification strategy using semicarbazide as Co-reaction accelerator for highly sensitive electrochemiluminescent aptasensor construction, Anal. Chem. 87 (2015) 11389–11397.
[28] B.J. Feng, H. Li, S. Meng, L. Chen, K.H. Wu, Structure and quantum well states in silicene nanoribbons on Ag (110), Sur. Sci. 645 (2016) 74–79.
[29] N. Yusoff, A. Pandikumar, R. Ramaraj, H.N. Lim, N.M. Huang, Gold nanoparticle based optical and electrochemical sensing of dopamine, Microchim. Acta 182 (2015) 2091–2114.
[30] W.J. Chen, L.Y. Zheng, M.L. Wang, Y.W. Chi, G.N. Chen, Preparation of protein-like silver-cysteine hybrid nanowires and application in ultrasensitive immunoassay of Cancer biomarker, Anal. Chem. 85 (2013) 9655–9663.
[31] T.Y. Huang, Q.M. Meng, G.F. Jie, Silver nanowires-based signal amplification for CdSe quantum dots electrochemiluminescence immunoassay, Biosens. Bioelectron. 66 (2015) 84–88.
[32] H.J. Wang, Y.L. Yuan, Y.Q. Chai, R. Yuan, Self-enhanced electrochemiluminescence immunosensor based on nanowires obtained by a green approach, Biosens. Bioelectron. 68 (2015) 72–77.
[33] C.Y. Xiong, H.J. Wang, Y.L. Yuan, Y.Q. Chai, R. Yuan, A novel solid-state $Ru(bpy)_3^{2+}$ electrochemiluminescence immunosensor based on poly(-ethylenimine) and polyamidoamine dendrimers as co-reactants, Talanta 131 (2015) 192–197.
[34] Q. Zhu, F.D. Cai, J. Zhang, K. Zhao, A.P. Deng, J.G. Li, Highly sensitive electrochemiluminescent immunosensor based on gold nanoparticles-functionalized zinc oxide nanorod and poly(amidoamine)-graphene for detecting brombuterol, Biosen. Bioelectron. 86 (2016) 899–906.
[35] Q. Zhu, J. Zhang, Q.H. Tang, K. Zhao, A.P. Deng, J.G. Li, Ultrasensitive electrochemiluminescent immunosensor for detecting brombuterol based on quantum dots-Graphene@Gold nanoparticles as signal enhancer, J. Electrochem. Soc. 163 (7) (2016) B352–B357.
[36] B.Y. Cao, G.Z. He, H. Yang, H.F. Chang, S.Q. Li, A.P. Deng, Development of a highly sensitive and specific enzyme-linked immunosorbent assay (ELISA) for the detection of phenylethanolamine A in tissue and feed samples and confirmed by liquid chromatography tandem mass spectrometry (LC–MS/MS), Talanta 115 (2013) 624–630.
[37] F. Lisdat, D. Schäfer, A. Kapp, Quantum dots on electrodes-new tools for bioelectroanalysis, Anal. Bioanal. Chem. 405 (2013) 3739–3752.
[38] P.P. Dai, T. Yu, H.W. Shi, J.J. Xu, H.Y. Chen, General strategy for enhancing electrochemiluminescence of semiconductor nanocrystals by hydrogen peroxide and potassium persulfate as dual coreactants, Anal. Chem. 87 (2015) 12372–12379.
[39] J. Zhang, F.D. Cai, A.P. Deng, J.G. Li, CdSe quantum dots based electrochemiluminescence immunosensor with simple structure for ultrasensitive detection of salbutamol, Electroanalysis 26 (2014) 1–9.
[40] R. Yaron, Y.K. Tal, D. Yael, F. Amihay, S.D. Yosi, Impact of molecular surface charge on biosensing by electrochemical impedance spectroscopy, Electrochim. Acta 200 (2016) 161–167.
[41] A. Ramanavicius, A. Finkelsteinas, H. Cesiulis, A. Ramanaviciene, Electrochemical impedance spectroscopy of polypyrrole based electrochemical immunosensor, Bioelectrochem 79 (2010) 11–16.
[42] A. Blomgren, C. Berggren, A. Holmberg, F. Larsson, B. Sellergren, K. Ensing, Extraction of clenbuterol from calf urine using a molecularly imprinted polymer followed by quantitation by high-performance liquid chromatography with UV detection, J. Chromatogr. A 975 (2002) 157–164.
[43] T.T. Dong, Q.H. Tang, M. Chen, A.P. Deng, J.G. Li, Ultrasensitive electrochemiluminescent competitive immunoassay for β-adrenergic agonist salbutamol based on quantum dots and enzymatic amplification, J. Electrochem. Soc. 163 (2016) B62–B67.